Dual-Polarization Radar Particle Classification Results during the Sochi Olympic Games

Janti Reid[1], David Hudak[1], Sudesh Boodoo[1], Norman Donaldson[1], Paul Joe[2], Dmitry Kiktev[3] and Aleksandr Melnichuk[4]

[1]*Science and Technology Branch, Environment Canada, King City, Canada*
[2]*Science and Technology Branch, Environment Canada, Toronto, Canada*
[3]*Hydrometcentre of Russia, Roshydromet, Moscow, Russia*
[4]*Central Aerological Observatory, Roshydromet, Dolgoprudny, Russia*
(Dated: 18 July 2014)

Janti Reid

1 Introduction

Weather forecasting in complex mountainous terrain during the 2014 Sochi Winter Olympic and Paralympic Games was supported by a number of meteorological advancements. These included a dense network of meteorological stations in the Sochi area, numerous international forecasting systems, innovative profiling temperature, wind and radar instrumentation, and a dual-polarized C-band Doppler radar on Akhun Mountain (Kiketv et al., 2013 and Kiktev, 2011). In conjunction with the Games, Forecast and Research in the Olympic Sochi Testbed (FROST-2014) was initiated as a World Meteorological Organization World Weather Research Program (WMO WWRP) project. One of its main objectives was the development and demonstration of modern forecast and nowcast systems in meteorological support of the Winter Olympics.

One of Environment Canada's (EC) contributions to FROST-2014 was the adaptation and implementation of a radar-based particle classification algorithm (PCA) for Akhun Radar. This algorithm, based on that developed by NOAA's National Severe Storm Laboratory (Park et al., 2009), is a fuzzy logic-based algorithm that exploits dual-polarimetric radar signatures to infer target particle type. The algorithm has been adapted for C-band wavelength and is currently operating in a real-time research environment at the King Radar Research Facility north of Toronto, Canada. A key component is the extent of the melting layer (ML) which provides restrictions on particle type classes above, inside and below the melting layer. PCA modifications for FROST-2014 focused mainly on the implementation of the melting layer determined from various sources. With sufficient radar returns, a radar-based melting layer algorithm (Giangrande et al., 2008 and Boodoo et al., 2010) was implemented as the first choice for ML as it provided azimuthally varying estimates of ML height and thickness. In this application an azimuthally averaged estimate of height and thickness was used. If the ML was undetectable by radar then the Canadian 250 m High Resolution Deterministic Prediction System (HRDPS) (Milbrandt et al., 2013) numerical model provided a single ML height and thickness to be used instead. The heights of the 0^{o}C level from upper air soundings were also used to compare to the radar and model derived melting heights.

The focus of the study is to validate the results of PCA at Akhun with observations collected during the Sochi Winter Games. Additionally the results are compared against those from Vaisala's HydroClass algorithm (HCA). The intent of this work is to verify the applicability of PCA in a complex geographical area.

2 Data Overview

2.1 Radar Data

Details of Akhun Radar, including the scan type analyzed in this study, are provided in Table 1. As a result of beam blockage from terrain, radar data from the second lowest elevation scan at 1.1° were selected to compare against surface observations. In this study we analyze the HIGH_PRF volume scan task which was scheduled regularly every 10 minutes.

Table 1: Summary of Akhun Radar and scan type analyzed in this study.

Radar Summary		Scan Summary	
Manufacturer/Model	Vaisala WRM200	Task name	HIGH_PRF
Processing software	IRIS version 8.13	Elevation angles	10 (0.3° to 32.5°)
Coordinates	43.548°N, 39.851°E	PRF	1000/750 Hz
Ground height	663 m	Rotation Rate/Samples	2.375 rpm; 50
Wavelength	5.33 cm	Pulse width	0.50 µs
Polarization	H+V	Data resolution	250 m by 1°
Beam width	0.95° / 0.95°	Maximum range	125 km

2.2 Surface Observations

Observation data were collected from surface present weather detectors (PWD) from 12 sites in Table 2 for the Sochi area. Their location in range and altitude relative to the radar and beam width are in Figure 1. Basic meteorological parameters including surface air temperature were also available. Precipitation type was identified by a Vaisala PWD22 present weather detector at the majority of the sites with the exception of KEP and SOL which used a PWD20 (see http://www.vaisala.com/en/roads/products/atmosphericsensors/Pages/PWDPresentweather.aspx for PWD22 technical specifications). Seven different types of precipitation types are distinguishable for the PWD22, namely rain, freezing rain, drizzle, freezing drizzle, mixed rain/snow, snow and ice pellets, at variable intensity. Observations were available every 10 minutes with intermittent periods of 20 minute observations at some sites.

Table 2: Summary of observation sites with present weather detectors.

	Site	Location (lat °N, lon °E)		Altitude (m ASL)	Range distance from Akhun (km)	Azimuth direction from Akhun (°)
SOL	Solokh-Aul	43.794	39.633	442	32	327.9
KEP	Kepsha	43.615	40.049	179	18	65.1
GC-1500	Gornaya Carousel-1500	43.660	40.251	1432	35	69.0
GC-1000	Gornaya Carousel-1000	43.668	40.257	978	35	67.9
SNO	Snowboard-1025	43.656	40.327	1025	40	72.6
FRE	Freestyle-1080	43.652	40.322	1075	40	73.1
SL-830	Sledge-830	43.662	40.287	835	37	70.1
SL-700	Sledge-700	43.669	40.289	701	38	69.2
SJ-800	Ski Jump-800	43.675	40.241	705	34	65.7
SJ-650	Ski Jump-650	43.676	40.241	630	35	65.6
BIAS	Biathlon Stadium	43.692	40.321	1455	42	67.3
LUN	Lunnaya Polyana	43.935	39.868	1804	43	1.8

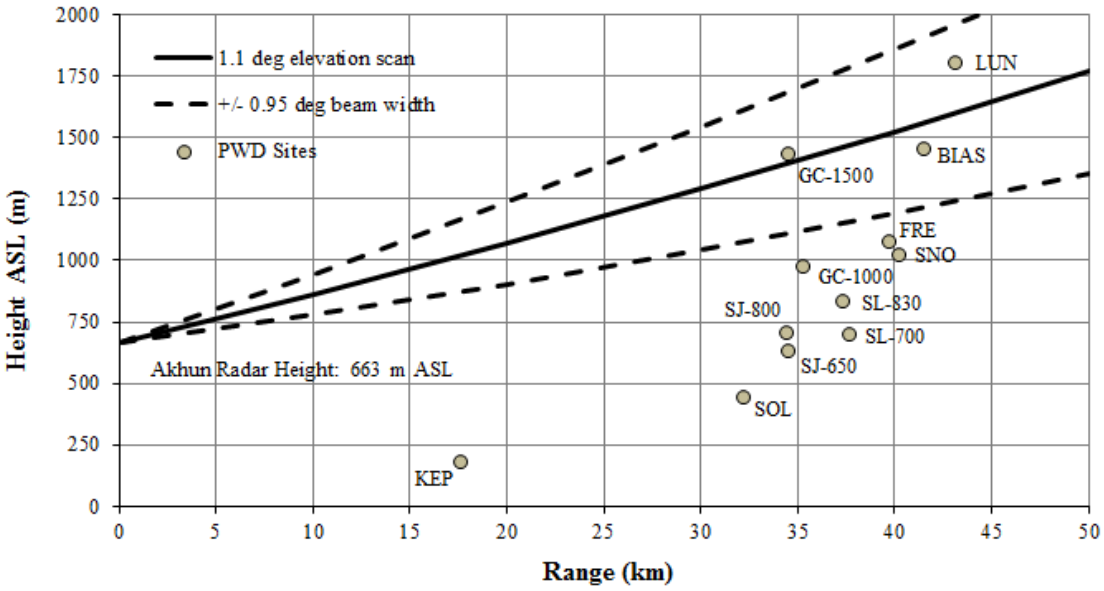

Figure 1: Elevation of present weather detector sites in relation to Akhun Radar's 1.1 ° elevation scan. Range indicates the distance between the site and Akhun Radar.

2.3 Upper Air Soundings

Upper air soundings were launched from less than 10 km northwest of the radar 4 times daily around 0, 6, 12 and 18 UTC. These data were specifically examined for freezing level heights that will be used in the comparison of melting layer heights in this study.

2.4 High Resolution Deterministic Prediction System (HRDPS) Numerical Model

Another EC contribution to FROST-2014 was the running of the HRDPS model by the Canadian Meteorological Centre (CMC) for the Sochi region. This experimental high resolution forecast system was also demonstrated at the 2010 Winter Games in Vancouver, Canada (Mailhot et al., 2012). In this work, 24 hour temperature forecasts from the 250 m resolution HRDPS are utilized by PCA. High time resolution model output, run once daily, was provided in 1 minute time intervals at specific sites including Akhun Radar.

2.5 Particle Classification Algorithm (PCA)

There are 11 PCA classification types: ground clutter or anomalous propagation (GC), biological (BIO), dry snow (DS), wet snow (WS), crystals (CR), graupel (GR), big drops (BD), rain (RA), heavy rain (HR), hail with rain (R/H) and unclassified (UN). PCA methodology can be broadly divided to three subsections: dual-polarization (D-P) data processing, melting layer determination and particle type classification. The input radar data required for PCA are: total power (T), ground clutter corrected reflectivity (Z), differential reflectivity (Z_{DR}), correlation coefficient (ρ_{HV}), differential phase (Φ_{DP}), specific differential phase (K_{DP}), radial velocity (V) and signal quality index (SQI). D-P data processing is composed of several data quality and data correction steps outlined in Table 3. It is noted that many of these steps are complete studies unto themselves, for example the attenuation correction of Z and Z_{DR}, and their full description is not provided here.

Table 3: D-P data processing steps.

1.	SQI thresholding
2.	Median filtering
3.	ρ_{HV} noise correction
4.	System Φ_{DP} calculation
5.	Φ_{DP} unfolding and smoothing
6.	Z and Z_{DR} attenuation correction
7.	SD(Z) and SD(Φ_{DP}) texture parameter calculation

Modifications of PCA for FROST-2014 focused on the implementation of a radar-based melting layer algorithm. In the research prototype running in Canada, PCA utilizes the height of the wet-bulb 0ºC level from a numerical weather model and a thickness defined by the height between wet-bulb temperatures at -0.2ºC and 3ºC for a model grid point closest to the radar. For Sochi, a similar model method was employed using the HRDPS, however, the model served as the secondary source for melting layer information when radar-based estimates were not available. In this work a default thickness of 500 m was used for the HRDPS method.

As described in Giangrande et al. (2008) and Boodoo et al. (2010), the radar-based algorithm estimates ML top and bottom as a function of azimuth. For Sochi, pixels from radial profiles between the 0.5° and 25° elevations were examined for possible melting using Z, Z_{DR}, ρ_{HV} and V. Melting pixel candidates were restricted to 20 dBZ < Z < 47 dBZ, 0.8 dB < Z_{DR} < 2.6 dB, 0.90 < ρ_{HV} < 0.97 and V > 1 m/s. Melting pixels were then boxcar filtered and the ML top was determined to be the height of the 80th percentile of the ML height distribution and the ML bottom from the 20th percentile. Finally the azimuthal ML heights and thickness results were averaged and a single mean height and thickness were used for the entire radar extent, similar to the model method. When there were insufficient echoes or when < 15% of radials had ML estimations, PCA used the ML from the secondary model source.

The post-processed D-P data and melting layer information are passed to the classification algorithm where pre-determined fuzzy logic trapezoidal membership functions and weighting factors determine the most likely particle type for each radar pixel (Park et al., 2009). These are combined in an additive manner; and the particle type with the highest likelihood value is deemed the winner. Additionally the position of the radar pixel in relation to the melting layer restricts the classification types that can be selected. For example, wet snow pixels are restricted to within the melting layer, all snow types are only available above the ML bottom and rain types are available below the ML top with exception of rain mixed with hail. The membership functions, weighting factors and classification restrictions used in this work are described in Park et al. (2009). The last step of the process applies final logical checks to re-classify any unreasonable results or low likelihood values.

2.6 HydroClass Algorithm (HCA)

The HydroClass product from Vaisala is derived from a collection of radar echo classification algorithms. The algorithms are described fully in the Vaisala Dual-Polarization and RDA User's Manual found at ftp://ftp.sigmet.com/outgoing/manuals/IRIS_and_RDA_Dual_Polarization_Users_Manual.pdf. In this work we evaluate the Meteo Classifier results (Liu and Chandrasekar, 2000) for which classes are rain (RA), wet snow (WS), snow (SN), graupel (GR), hail (HA), non-meteorological (NM) and no data. One notable difference between HCA and PCA is the inclusion of altitude-based membership functions that have a dependence on the provided melting layer height. PCA does not include this in its algorithm.

3 Data Analysis and Validation

Four precipitation cases were selected during the Olympic and Paralympic period for analysis:

1. Feb 17 1905 UTC – Feb 18 2355 UTC

2. Feb 20 1605 UTC – Feb 21 1355 UTC
3. Feb 26 0005 UTC – Feb 28 2355 UTC
4. Mar 10 2305 UTC – Mar 12 2355 UTC

On Feb 17 precipitation entered the Sochi area from the northwest. At the end of the event, FROST-2014 bloggers reported > 30 cm of snow at the 2 km level at Rosa Khutor mountain. A non-symmetric bright-band signature was evident in the radar PPI product (i.e. a "ring" of low (red) ρ_{HV} values; see Figure 2a) indicating a slanting melting layer as also seen in the ρ_{HV} cross-section (Figure 2b). On Feb 20 precipitation arrived from the northwest and bloggers noted intense rain showers at the Rosa Khutor Finish (980 m) between 6-8 UTC on the 21st. Feb 26 and March 10 events were longer and originated from the southeast over the Black Sea and then later on from the southwest. Orographic factors contributed to the enhanced precipitation in the Olympic region for those cases.

(a) ρ_{HV} PPI for 3.1°

(b) ρ_{HV} cross-section along 255° / 75° radial

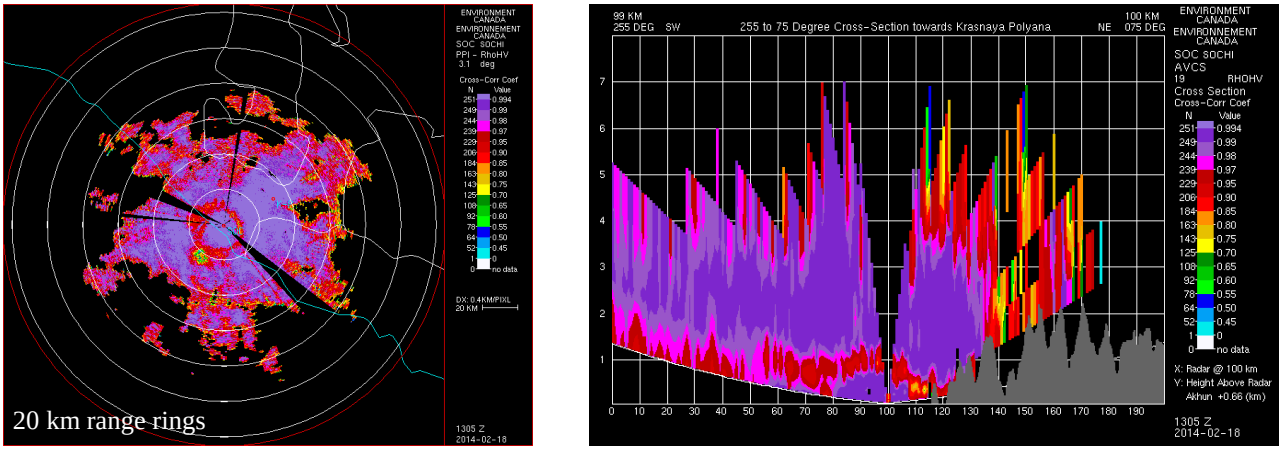

Figure 2: Feb 18 1305 UTC ρ_{HV} (a) PPI for 3.1° and (b) cross-section along 255°-75°. The non-symmetric ring of low (red) ρ_{HV} values seen inside the first 20 km range ring indicates a slanting melting layer. This is evident in (b) as low ρ_{HV} values are lower in height towards the mountains. The "sagging" of the melting layer in (b) suggests a radar antenna pointing error.

3.1 Melting Layer Comparison

Melting layer heights from the radar-based algorithm (blue diamonds), HRDPS (green triangles) and UA (red dots) are plotted for each case in Figure 3. Melting levels from HRDPS and UA were calculated by finding the highest freezing level in their respective profiles. For the Feb 17 and 20 cases, PCA underestimated the melting layer and considerably so at times, while the HRDPS generally had a smaller upward bias compared to the UA. The lack of sufficient radar echoes also disallowed radar-based melting layers for significant periods for these two cases. Since PCA uses ML to help discriminate particle types, most notably between rain and snow, its importance cannot be understated. Challenges for PCA occurred when successive radar scans alternated between the model and radar-based algorithm and the result was a visible "jump" in precipitation type with range (corresponding to height in a radar PPI product). Figure 4 depicts a sequence of PCA PPI scans between 2305 and 2335 UTC on Feb 17. At 2305 PCA uses the model ML at 1.6 km ASL with 0.5 km thickness. At 2215 (not shown) and 2225 PCA selects the radar-based ML with a lower 1.0 km height and thinner 0.1 km thickness and then back to model at 2235 with a 1.6 km height ML. The result of this discrepancy is a dramatic shift in the rain-snow classification boundary. Other discontinuities in the data, such as a change in model forecast runs at Feb 21 at 0 UTC (Figure 3b), also affected particle type output. For the Feb 26 and Mar 10 cases, PCA properly captures the drop in the melting layer. HRDPS similarly captures the drop and compares well with the sounding data. In all cases PCA is seen to underestimate ML heights as compared to the sounding information.

(a) Feb 17

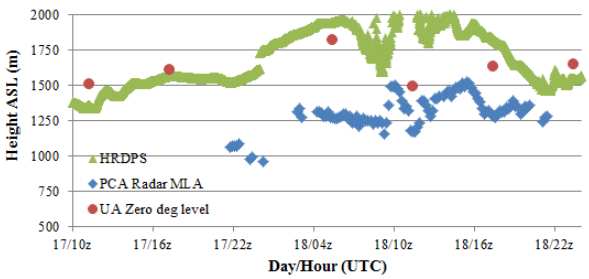

(b) Feb 20

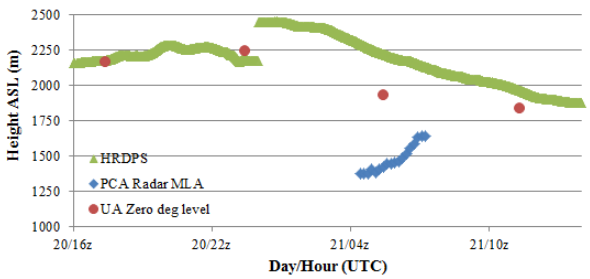

(c) Feb 26 (d) Mar 10

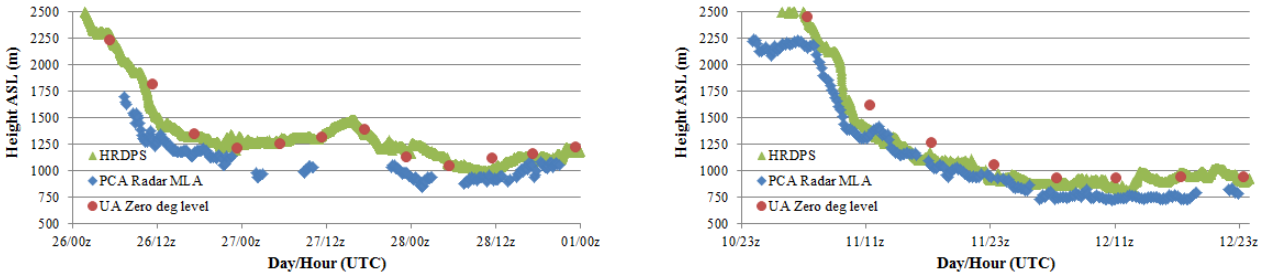

Figure 3: Melting layer height derived by HRDPS (green), PCA radar-based melting layer detection algorithm (blue) and upper air soundings (red). Melting layer height from HRDPS and UA are the height of the highest 0ºC level.

(a) PCA at 2305 UTC (b) PCA at 2325 UTC (c) PCA at 2335 UTC

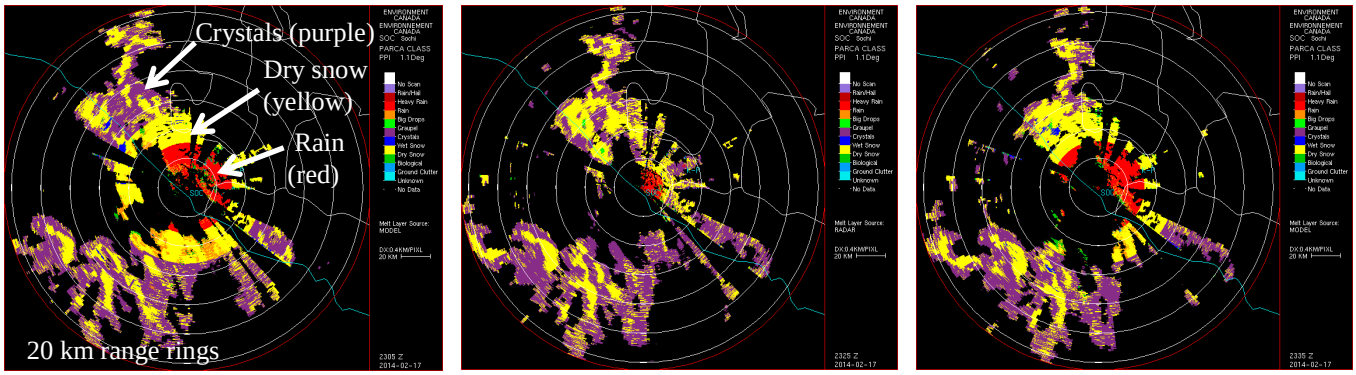

Figure 4: Sequence of PCA results for 1.1º scan on Feb 17. Changes in the melting layer height directly affect the selection of snow (dry snow – yellow, crystals – purple) and rain type (red).

3.2 Particle Type Validation for Rain, Snow and Rain/Snow Mix

Data for the validation were organized in the following manner: HIGH_PRF radar scans were available every 10 minutes and the closest PWD and temperature observations in time were matched with the corresponding radar scan. If the time difference between the radar and the observations was greater than 20 minutes then the observations were tagged as not available. For the purposes of this study, the types of observed precipitation were further reduced those in Table 4. The comparison of radar particle type inference to surface observations is complicated by the radar particle class categories not directly matching those from observations. During the Games, rain, snow and rain/snow mix were the predominant types observed and thus this work focuses on the validation of these 3 types.

Table 4: Observed particle classification types.

None
Drizzle (DZ)
Rain (RA)
Freezing Rain (FZRA)
Mix of rain and snow (R/S)
Snow (SN)
Ice pellets (IP)

To validate the results of the 1.1º scan with the available PWD data, a sector of radar data between the 65º and 75º azimuth angles was selected to cover the spatial area with largest number of PWD sites (9 excluding KEP; see Table 2). Different heights of the elevation scan were evaluated by separating altitudes into 250 m bins: 500 – 750 m, 750 – 1000 m, 1000 – 1250 m and 1250 – 1500 m above sea level. With this configuration at least 2 sites were represented in each height bin (see Figure 1). For each radar scan, if there was a rain or snow or rain/snow observation at a given site (corresponding to a particular height bin), PCA and HCA pixels within the 65º-75º sector for altitudes within that height bin were also extracted. The result is a distribution of PCA and HCA particle classification types at 4 levels which can be validated against ground-truth values of rain, snow and rain/snow at those elevations. One caveat of this validation method is that radar pixels for the lower elevations are from ranges closer to the radar as compared to the actual range of the corresponding PWD site (see Figure 1) for which the particle type was observed. So the assumption here is that the temperature profile is relatively uniform across the study area. This is not always the case (see Feb 17 case in Figure 2). Another concern was evaluating radar pixels that are in dissimilar geographic conditions as the observing site. This is mitigated somewhat by choosing the 11º mountainous sector that covers most of the sites and which would restrict the inclusion of pixels over, for example, the Black Sea. It does not however address local orographic-related phenomena that exist in this complex terrain.

Results were tabulated over all four cases in Table 5. Percentage of occurrence of each particle type is given and it is noted that the occurrence of unclassified and no data radar pixels from PCA and HCA, respectively, have been removed from the percentage calculations. Surface temperatures were also collected and stratified.

(a) Distribution of observed particle type and surface temperatures

Height m ASL	DZ	RA	FZRA	R/S	SN	IP	Min T (ºC)	Max T (ºC)	Avg T (ºC)	Std T (ºC)
1250-1500	0%	23%	1%	9%	66%	1%	-3.9	8.3	-0.4	2
1000-1250	2%	59%	0%	19%	21%	0%	-0.9	6.6	1.2	1.6
750-1000	5%	73%	0%	9%	13%	0%	-0.5	11.6	2.4	1.8
500-750	5%	90%	0%	4%	1%	0%	0.7	8.4	3.9	1.6

(b) Distribution of PCA particle types

Height m ASL	GC	BIO	BD	RA	HR	WS	DS	CR	GR	R/H
1250-1500	1%	8%	4%	15%	0%	3%	32%	38%	0%	0%
1000-1250	1%	12%	8%	27%	0%	5%	19%	28%	0%	0%
750-1000	0%	13%	10%	52%	0%	6%	9%	10%	0%	0%
500-750	1%	11%	12%	70%	0%	3%	3%	0%	0%	0%

(c) Distribution of HCA particle types

Height m ASL	NM	RA	WS	SN	GR	HA
1250-1500	16%	16%	17%	51%	1%	0%
1000-1250	17%	22%	26%	34%	2%	0%
750-1000	17%	37%	31%	15%	1%	0%
500-750	18%	40%	31%	11%	1%	0%

Table 5: Distribution of particle types by height from (a) PWD observations, (b) PCA and (c) HCA for times when rain, snow or rain/snow PWD particle types were observed. The corresponding distribution of observed surface temperatures is also given in (a).

At 1250-1500 m PCA identified 70% of the classified targets as snow (32% DS + 38% CR) compared to 66% PWD snow-only observations. HCA determined 51% of the targets as snow-only. If wet snow and observed rain/snow mix are added to these percentages, PCA identifies 73% as snow (32% DS + 38% CR + 3% WS), 75% for PWD (66% SN + 9% R/S) and 68% for HCA (51% SN + 17% WS). The validation of WS from radar is complicated as there is no true matching PWD category. At 500-750 m PCA identified 82% as rain (12% BD + 70% RA) compared to 90% PWD rain-only observations. HCA inferred 40% as rain-only. With respect to determining snow at higher altitudes and rain lower in height, the distribution of PCA types compared reasonably with observations.

A notable difference between PCA and HCA is the percentage of wet snow bins where HCA tends to identify more WS pixels over PCA by a factor of 5 to 10. An example is depicted in Figure 5 for Feb 26 at 1755 UTC. For this case the radar-based ML was 1.2 km with a thickness of only 0.1 km. The freezing level from the 1725 UTC sounding was 1.35 km. The melting level provided to HCA in the IRIS system was 1.9 km which seems represented by a rough boundary between wet snow (blue) and snow (yellow) at just beyond the 40 km range in Figure 5b. Even if the ML thickness was underestimated by PCA, one might still expect more rain classification at lower ranges (altitudes) for HCA as compared to wet snow. At 1755 UTC surface temperatures at SJ-800, SJ-650 and SL-700 were 4.8°C, 5.1°C and 5.0°C, respectively, and as expected, rain was observed at these heights. At higher altitudes temperatures were 3.9°C, 3°C, 2.5°C and 1.9°C for SL-830, GC-

1000, SNO and FRE, respectively. Each of these sites reported rain at that time. Since the initial HCA melting level was high (1.9 km) and not unreasonable, the problem instead points at the fuzzy logic membership and weighting functions as the source of the substantial wet snow classifications. In contrast, PCA may be seen as inferring unrealistically low amounts of wet snow pixels (3-6% for all height bins). Once again it is difficult to validate wet snow given the PWD type categories.

(a) PCA on Feb 26 1755 UTC (b) HCA on Feb 26 1755 UTC

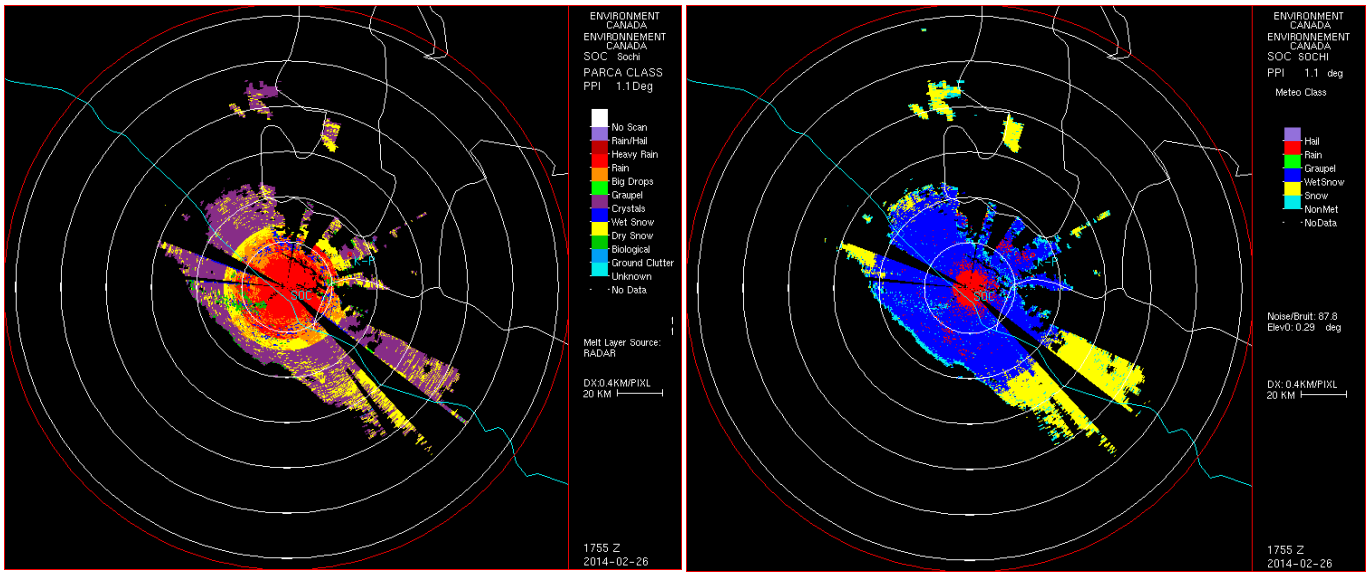

Figure 5: (a) PCA and (b) for 1.1º scan on Feb 26 1755 UTC. HCA classifies more pixels as wet snow (blue) compared to rain (red).

4 Summary & Future Work

A description has been provided of a radar particle classification system demonstrated during the Sochi Olympic Winter Games. Melting layers derived from a radar-based detection algorithm follow the trend of the freezing level from upper air soundings for at least 2 cases when precipitation occurred for a considerable period. The system is challenged when it switches, sometimes abruptly, between melting layer sources and future work should include provisions for a smoother transition and improved logic in selecting between sources. For all cases, the radar-based melting layer is lower than the UA freezing level. There is evidence of radar antenna pointing errors for Akhun Radar as seen by a "sag" in the bright-band in cross-sectional products.

In analyzing the 1.1º elevation scan, the PCA compared well with rain and snow surface observations at 500-750 m and 1250-1500 m ASL heights, respectively. Wet snow validation is not directly verifiable against PWD observations, however, it appears that HCA can overestimate wet snow compared to rain in the snow-to-rain transition in the lower melting layer and that PCA unrealistically underestimates wet snow, particularly in the rain-to-snow transition near the top of the melting layer. In the future, particle type validation can be furthered by examining vertically profiling Micro Rain Radar (MRR) data from 2 Sochi-area sites. Melting layer information and fall speeds from the MRR may help discern particle type. These data are anticipated to become available shortly.

The King Radar Research Facility is currently working towards improvements in D-P pre-processing (e.g. attenuation and noise corrections, KDP calculation, non-uniform beam-filling, etc.) and any advancement here will benefit PCA. Additionally, the use of a 2D model temperature field for PCA is planned for implementation.

Environment Canada is presently upgrading ten of its radars to dual-polarization by 2015-2016 as part of its Radar Renewal Project. Plans are underway to operationally implement PCA and related D-P radar science. This study suggests that PCA can be applicable in mountainous regions and regional tuning of membership and weighting functions would likely improve PCA results.

Acknowledgements

The authors would like to thank Anna Glazer from CMC/EC for her work with the HRDPS and in particular with her setup of the high time resolution time series version of the 250 m forecast model. The authors would also like to thank the Sochi Olympic Forecasters and FROST-2014 team for their interest and feedback regarding radar science and products leading up to and during the Games. Additionally comments posted on the FROST-2014 blog page (visit http://frost2014.meteoinfo.ru/sochi_blog/), particularly those from Larisa Nikitina, were invaluable for capturing the essence of weather events during the Games.

References

Boodoo, S., Hudak D., Donaldson N. and Leduc M. Application of Dual-Polarization Radar Melting-Layer Detection Algorithm. *Journal of Applied Meteorology and Climatology*, 2010, Vol 49, pp. 1779-1793. DOI: 10.1175/2010JAMC2421.1.

Giangrande, S., Krause J. and Ryzhkov A. V. Automatic designation of the melting layer with a polarimetric prototype of the WSR-88D radar. *J. Appl. Meteor. Climatol.*, 2008. 47, pp. 1354–1364.

Kiktev D. FROST-2014: Forecast and Research in the Olympic Sochi Testbed. THORPEX European Regional Meeting, 24-27 May 2011. Karlsruhe, Germany.

Kiktev, D. B., Astakhova E. D., Blinov D. V., Zaripov R. B., Murav'ev A. V., Rivin G. S., Rozinkina I. A., Smirnov A. V. and Tsyrul'nikov M. D. Development of Forecasting Technologies for Meteorological Support of the Sochi-2014 Winter Olympic Games. ISSN 1068-3739, *Russian Meteorology and Hydrology*, 2013, Vol. 38, No. 10, pp. 653–660.

Liu, H. and Chandrasekar V. Classification of Hydrometeors Based on Polarimetric Radar Measurements: Development of Fuzzy Logic and Neuro-Fuzzy Systems, and In Situ Verification. *J. of Atmospheric and Oceanic Technology*, 2000. 17.2, pp. 140-164. DOI: http://dx.doi.org/10.1175/1520-0426(2000)017<0140:COHBOP>2.0.CO;2.

Mailhot, J., Milbrandt, J.A., Giguère, A., McTaggart-Cowan, R., Erfani, A., Denis, B., Glazer, A. and Vallée M. An Experimental High-Resolution Forecast System During the Vancouver 2010 Winter Olympic and Paralympic Games. *Pure Appl. Geophys.*, 2012. DOI: 10.1007/s00024-012-0520-6.

Milbrandt J., Bélair, S. and Glazer A. Environment Canada's High Resolution Deterministic NWP System for FROST-14. 3rd FROST-2014 Meeting, 10-12 April 2013. St. Petersburg, Russia. **Park, H., Ryzhkov A. V., Zrnić D. S. and Kim K-E.** The Hydrometeor Classification Algorithm for the Polarimetric WSR-88D: Description and Application to an MCS. *Weather and Forecasting*, 2009. 24:3, pp. 730-748.